FULL PAPER

Gold Functionalized Mesoporous Silica Nanoparticle Mediated Protein and DNA Codelivery to Plant Cells Via the Biolistic Method

Susana Martin-Ortigosa, Justin S. Valenstein, Victor S.-Y. Lin, Brian G. Trewyn, and Kan Wang**

This article is dedicated to the memory of Professor Victor S.-Y. Lin, deceased May 4, 2010, in recognition of his inspiration and friendship

The synthesis and characterization of a gold nanoparticle functionalized mesoporous silica nanoparticle (Au-MSN) platform for codelivery of proteins and plasmid DNA to plant tissues using a biolistic particle delivery system is reported. The in vitro uptake and release profiles of fluorescently labeled bovine serum albumin (BSA) and enhanced green fluorescent protein (eGFP) are investigated. As a proof-of-concept demonstration, Au-MSN with large average pore diameters (10 nm) are shown to deliver and subsequently release proteins and plasmid DNA to the same cell after passing through the plant cell wall upon bombardment. Release of fluorescent eGFP indicates the delivery of active, non-denatured proteins to plant cells. This advance represents the first example of biolistic-mediated codelivery of proteins and plasmid DNA to plant cells via gold-functionalized MSN and provides a powerful tool for both fundamental and applied research of plant sciences.

1. Introduction

Recent advancements in the synthesis of monodispersed, large average pore diameter mesoporous silica nanoparticle (MSN) materials with highly functionalizable surface area (≥400 $m^2 g^{-1}$) and pore volume (1.05 $cm^3 g^{-1}$) has led to the development of a series of biomolecule delivery vehicles, where various proteins, small DNA and RNA sequences, and other biomolecules are loaded into the mesopores and on the external surface, and released in vitro or in cellular systems.[1–4] The large pore volumes and surface area of these materials allow for the efficient adsorption of biomolecules and subsequent delivery to viable animal and plant cells. Additionally, recent reports on functionalizing the surface of MSN demonstrate that this material can be tuned to optimize various applications. Organic and inorganic functionalization leads to control in MSN uptake by cells,[5] magnetization of MSN,[6] the DNA/RNA affinity for MSN,[7] and increasing the inherent density of MSN.[3] These examples illustrate the potential that MSN materials have on biomolecule entrapment and release applications.

Delivery of biomolecules mediated by MSN materials is particularly interesting because proteins are often unable to cross the membrane barrier of cells without the assistance of protein transport systems.[8] Several proteins have been successfully loaded and released from MSN materials,[9–13] however; only one example demonstrated the in vivo release of active protein from MSN in a mammalian cell system and no protein delivery to plant cells has been reported.[14]

There are few methods for protein delivery to plant cells, none of them nanoparticle mediated, including microinjection[15,16] and cell-penetrating peptides.[17–19] While these methodologies have been used to introduce model proteins into plant cells, they require the skillful handling of cell materials and lack the protection needed for the introduced protein during the process. Recently, using 1 μm gold microparticles, Wu et al. delivered a DNA-enzyme complex into plant cells through the biolistic method. The codelivery of the complex led to enhanced plant transformation efficiency but required covalent modification of the protein so it would remain attached to the gold microparticle during bombardment.[20]

Delivery of proteins or codelivery of proteins and DNA to plant cells has great biological significance. In addition to the potential of enhancing genetic transformation and gene targeting in plants,[20] researchers can assess the loss or gain of function of different post-translationally modified forms of a protein, and protein interactions with other biomolecules. Also, direct delivery and release of proteins in plant cells could

Dr. S. Martin-Ortigosa, Prof. K. Wang
Center for Plant Transformation
Plant Sciences Institute
Department of Agronomy
Iowa State University, Ames, IA 50011, USA
E-mail: kanwang@iastate.edu
Dr. J. S. Valenstein, Prof. V. S.-Y. Lin, Prof. B. G. Trewyn
Department of Chemistry
U.S. Department of Energy Ames Laboratory
Iowa State University, Ames, IA 50011, USA
E-mail: bgtrewyn@iastate.edu

DOI: 10.1002/adfm.201200359

facilitate the understanding of cellular machinery or signal pathways more effectively. This would lead to greater understanding of protein functions in host cells where protein production pathways are impaired; or analyzing cellular regulatory functions through delivery of antibodies.[20–23]

To date, nanoparticle-mediated delivery of biogenic molecules to plant cells has been limited to nucleic acids, including double or single stranded DNA[3,24–28] and small interfering RNA.[29] Delivery and release of chemical substances such as phenanthrene and plant growth regulators have also been reported.[30,31] Using the interior pore volume and the exterior surface of MSN along with particle bombardment technology, we previously demonstrated that plasmid DNA carrying a chemically inducible marker gene encoding for green fluorescent protein (GFP) and a chemical inducer (β-oestradiol) could be co-delivered to plant tissues.[3] The controlled release of *β*-oestradiol led to the expression of GFP in plant cells.[3] Additionally, in recently published work, we demonstrated that MSN delivery to plants through the biolistic method is improved by increasing the density of MSN by gold functionalization; leading to an enhanced cell penetration and subsequent DNA expression.[26]

In this work, we report the modified synthesis and characterization of a previously published gold functionalized, large pore diameter MSN (Au-MSN).[32] The in vitro uptake and release profiles of fluorescently labeled bovine serum albumin (BSA) and enhanced green fluorescent protein (eGFP) by Au-MSN are reported. Protein loaded Au-MSNs were coated with plasmid DNA following our DNA precipitation method.[26] The codelivery of plasmid DNA and proteins into plant cells using the biolistic method are achieved. The expression of the marker genes and the release of fluorescent proteins can be detected in the same plant cells one day after the bombardment. We demonstrated, for the first time, successful protein delivery and DNA/protein codelivery to plant cells mediated by Au-MSN as depicted in **Figure 1**.

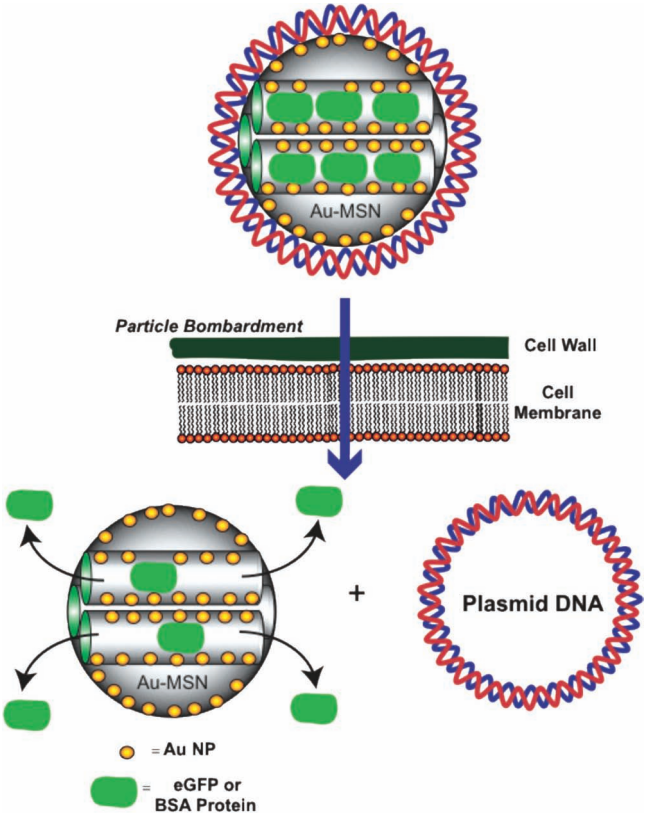

Figure 1. Schematic representation of Au-MSN mediated codelivery of proteins and plasmid DNA to plant cells via particle bombardment.

2. Results and Discussion

2.1. MSN Material Synthesis and Characterization

The synthesis of Au-MSN material was modified from a previous publication by Dai and co-workers[32] and completed according to the protocol described in our previous work.[26] Nitrogen sorption analyses, electron microscopy measurements, and powder X-ray diffraction (XRD) spectroscopy were utilized to fully characterize the Au-MSN materials that were synthesized by repeated gold reduction on the surface of the MSN. The repeated surface gold reduction was necessary to increase the nanoparticle density for successful delivery to plant cells by bombardment.[26] The Au-MSN exhibited a type IV isotherm with a BET surface area of 313 m^2 g^{-1} and a pore volume of 0.89 cm^3 g^{-1} and the BJH pore size distribution measurement showed a negligible decrease in pore diameter after three cycles of gold reduction (Figure S1, Supporting Information). As is observed in the transmission electron microscopy (TEM) image (**Figure 2**a and Figure S2, Supporting Information), the pore channels can be seen as parallel stripes running the length of the MSN, confirming the XRD pattern of a well ordered material. The scanning transmission electron microscopy (STEM) image (Figure 2b and Figure S3a, Supporting Information) shows the presence of gold nanoparticles on the surface of Au-MSN after the repeated deposition and reduction of gold salt. Scanning electron microscopy (SEM) image shows that the structure, shape and size of Au-MSNs are around 600 nm in diameter and have consistent particle size and morphology (Figure 2c). Energy dispersive X-ray analysis confirms that presence of gold on the surface of the MSN (Figure S3b, Supporting Information). The X-ray diffraction pattern of the Au-MSN material indicates a well-ordered pore structure characteristic of 2D hexagonal MSN (Figure 2d). High angle XRD patterns of MSN and Au-MSN confirm the presence of crystalline gold on the MSN (Figure S4, Supporting Information). The overall surface charge of each sample was measured in pH 7.4 PBS. The zeta potential of the MSN-10 (-29.0 mV) decreased slightly after gold was reduced on the surface to form Au-MSN (–25.5 mV). Measuring the zeta potential of plasmid DNA coated Au-MSN proved to be difficult due to significant particle aggregation during the surface charge measurement acquisition. To verify the synthesis of MSN-10 is consistent and the particle morphology and size is conserved, SEMs were recorded from four different batches. These SEMs are included in the supporting information (Figure S5, Supporting Information).

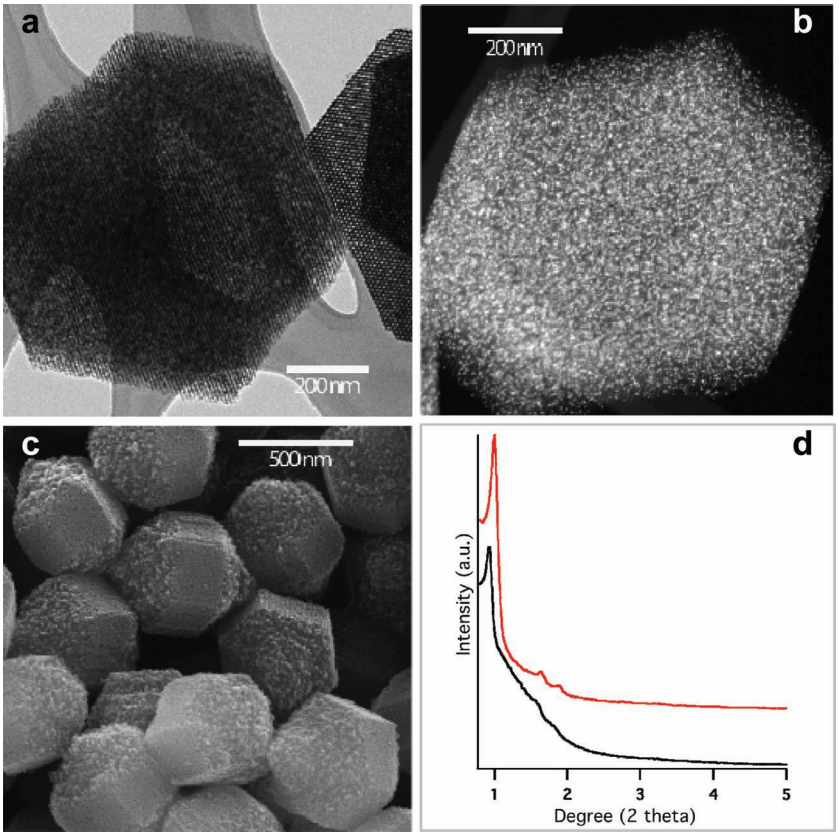

Figure 2. TEM image (a), STEM image (b) and SEM image (c) of Au-MSN. X-ray diffraction patterns of MSN (red) and Au-MSN (black) (d). TEM and STEM images were obtained using a Tecnai F^2 microscope and the SEM was obtained using a Hitachi S4700 FE-SEM system with a 10 kV accelerating voltage.

2.2. Au-MSN Protein Loading and In Vitro Release

As a proof-of-concept, two different proteins were chosen for Au-MSN loading (**Table 1**): BSA, fluorescein isothiocyanate (FITC-BSA) labeled or tetramethyl rhodamine isothiocyanate (TRITC-BSA) labeled and eGFP. The size of these proteins (hydrodynamic radius of 4.5 and 2.3 nm for BSA and eGFP, respectively)[33,34] was smaller than the 10 nm diameter pore size of the Au-MSN (Table 1). Therefore, high protein loading into the pores was expected.[35] As is described in detail in the experimental section, the amount of each protein that was entrapped in the mesopores was determined by measuring the difference in protein concentration in the supernatant before and after the loading procedure. Our measurements indicated that the maximum protein loading, at the conditions studied, was 625 and 150 mg of protein per 1.0 g of Au-MSN for FITC-BSA and eGFP, respectively (Table 1).

After the proteins were loaded in the Au-MSN, a time course of in vitro release of the loaded proteins was performed at room temperature during which the structure and activity of the proteins were maintained as is evident by continued fluorescence of the released eGFP.[36] The fluorescently-labeled BSAs showed a continuous release pattern during the first 20 h, while the eGFP achieved maximum release after 10 h (**Figure 3**). The difference in release kinetics could be attributed to the variation in the amount of protein loaded in the Au-MSN, the difference in protein-pore wall interaction, and the difference in the sizes of eGFP and BSA (Table 1). After 48 h incubating at room temperature (22 °C) in static conditions in phosphate buffered saline (PBS) solution (pH 7.4), the total percent of protein released was 28% and 8% for BSA and eGFP, respectively. Improving and controlling the percentage of protein release are research activities currently in progress. Subsequent suspension of the protein loaded Au-MSN pellets for further protein release did not yield more fluorescence in the supernatant, suggesting that no more detectable free proteins were released from the MSN (data not shown).

Table 1. Protein and protein loaded Au-MSN characteristics.

Protein	Size [kDa]	R_h[a)] [nm]	pI	Protein/ Au-MSN [mg g^{-1}]	% protein released
BSA	66.8	4.5	4.7	625	28
GFP	28	2.3	6.2	150	8

[a)] R_h is the hydrodynamic radius.[33,34]

2.3. Au-MSN Mediated Protein Delivery to Plant Cells

To introduce protein-encapsulated Au-MSN to plant cells, we used the biolistic delivery method as previously reported.[3,26] Release of FITC-BSA was observed in bombarded onion epidermis cells as early as 30 min after bombardment (**Figure 4**a). Nevertheless, protein release was typically observed 1 day after bombardment as in the case of eGFP (Figure 4b). In general, fluorescently-labeled BSA release was more distinguishable and

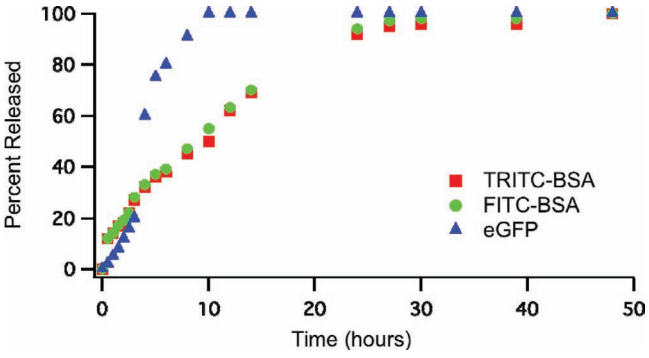

Figure 3. Normalized release profiles of FITC-BSA (green), TRITC-BSA (red), and eGFP (blue) from Au-MSN in pH 7.4 PBS solution.

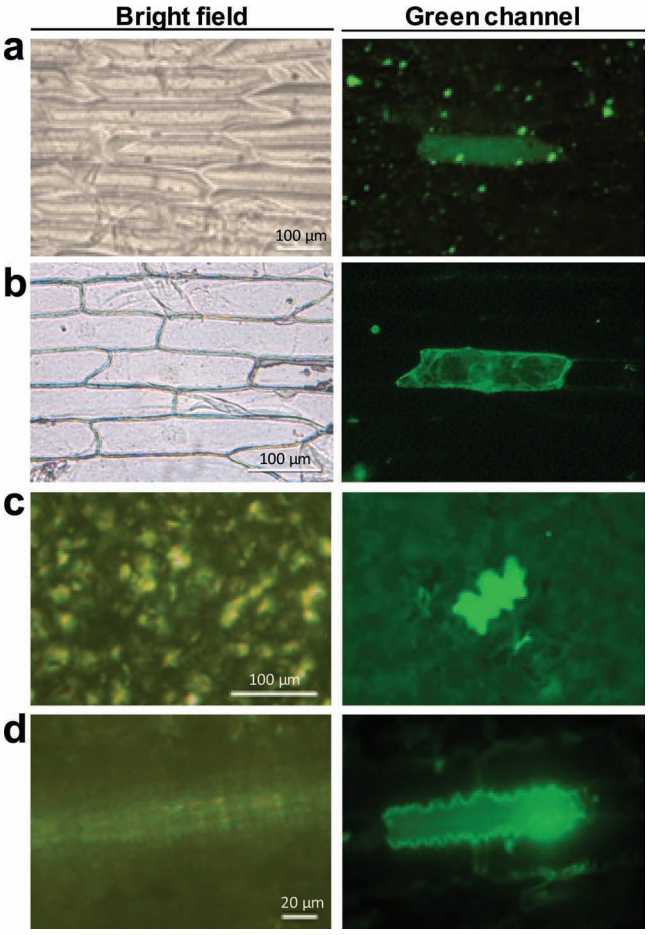

Figure 4. Delivery of proteins into plant tissues. Bright field and green channel images of a) onion epidermis cells showing FITC-BSA release 30 min after bombardment. b) Intracellular release of eGFP in onion epidermis cells one day after bombardment. Tobacco (c) or teosinte (d) leaf cell showing FITC-BSA release one day after bombardment.

more frequent than eGFP detection. A typical bombardment for fluorescently labeled BSA release showed hundreds of fluorescent onion epidermis cells, while eGFP release occurred in less than 10 cells per bombarded sample (2 cm × 3.5 cm in size). This difference could be due to the smaller amount of protein encapsulated into Au-MSN, the lower release percentage (Table 1) and the overall lower fluorescence emission of eGFP comparing to FITC-BSA.[37] Although limited eGFP release could be observed in a small number of cells one day after the bombardment, longer periods of time (up to 6 days) were needed to obtain more fluorescent cells, likely due to continued release of eGFP from Au-MSN in plant cells over time.

To prove this system is applicable in other plant tissues, leaves of tobacco and teosinte plants were bombarded as described for onion epidermis tissue. In both cases (Figure 4c,d, respectively) cells showing FITC-BSA release were found in the plant tissues one day after bombardment. In the plant tissues tested, the fluorescence was observed throughout the cell, not localized in cell compartments, indicating that the fluorescent proteins were released into and diffused throughout the cell cytoplasm (Figure 4a–d).

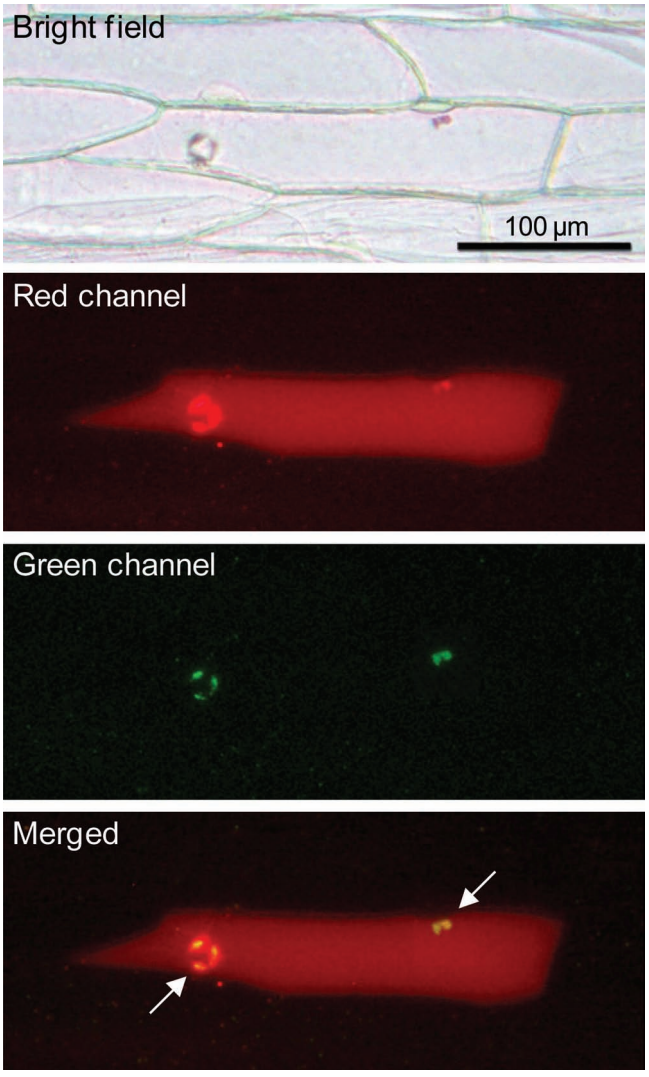

Figure 5. Association of Au-MSN and protein release in plant cells. Bright field, red channel, green channel, and merged images of an onion cell 1 day after bombardment with TRITC-BSA loaded, FITC labeled Au-MSN. White arrows point at Au-MSN clusters.

To confirm that the observed cellular fluorescence is due to MSN introduction and not to isolated protein aggregates formed during MSN-loading, we covalently labeled Au-MSN with FITC prior to TRITC-BSA protein encapsulation. Onion epidermis cells bombarded with this material showed red fluorescent cells (due to TRITC-BSA release) and green fluorescent dots (FITC-labeled Au-MSN), confirming that the TRITC-BSA release is associated with the presence of Au-MSN inside the same plant cell (**Figure 5**).

2.4. Au-MSN Mediated Codelivery of Protein and Plasmid DNA to Plant Cells

Simultaneous delivery of plasmid DNA and protein in onion epidermis cells is shown in **Figure 6**. For DNA coating and delivery of protein-encapsulated Au-MSN, we used a recently

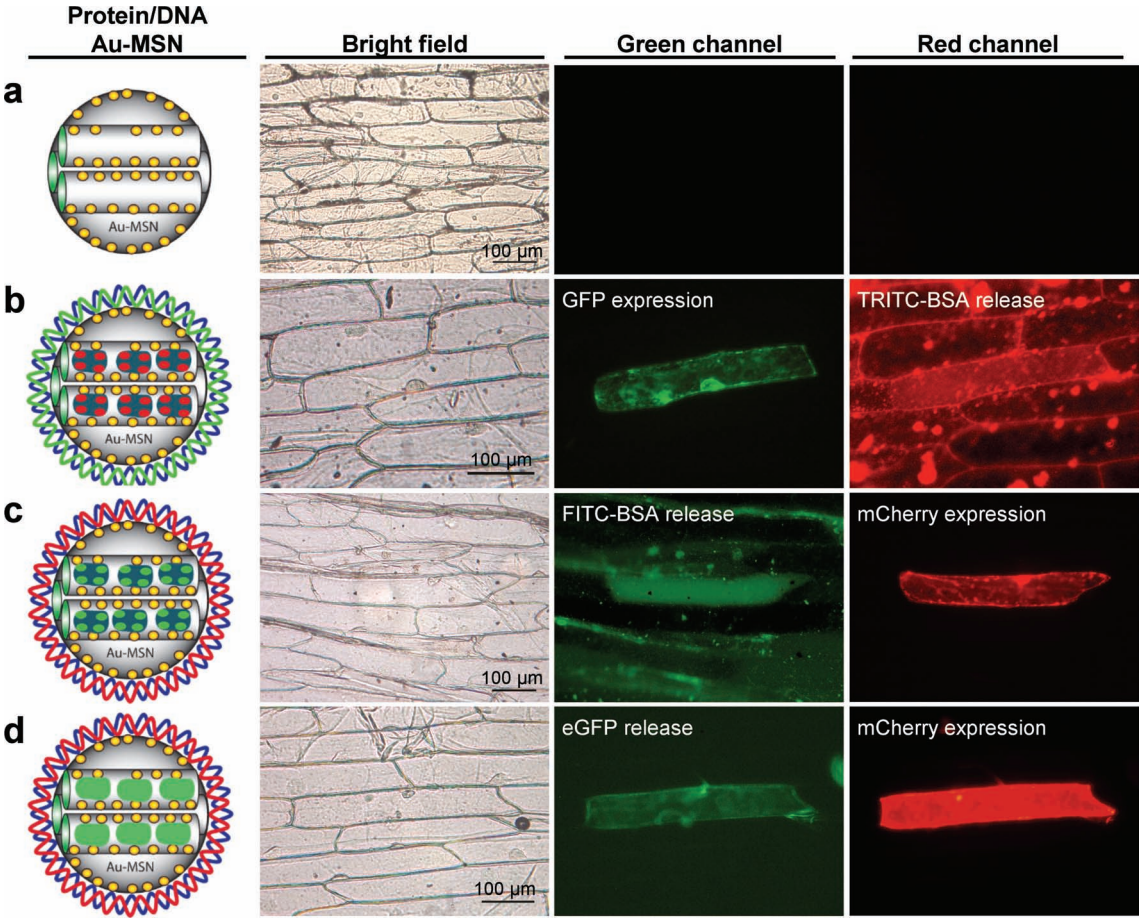

Figure 6. Bright field, green channel, and red channel fluorescent microscopy images of onion epidermis cells bombarded with empty Au-MSN (a), TRITC-BSA protein loaded and GFP expressing plasmid DNA coated Au-MSN (b), FITC-labeled BSA protein loaded and mCherry expressing plasmid DNA coated loaded Au-MSN (c), and eGFP protein loaded and mCherry expressing plasmid DNA coated Au-MSN (d).

optimized biolistic procedure for Au-MSN.[26] The plasmids used were ER-rk[38] (red fluorescent protein mCherry gene expression) when FITC-BSA or eGFP loaded Au-MSN were used, and pLMNC95[39] (GFP gene expression) for TRITC-BSA loaded Au-MSN. The co-localization of both red and green fluorescent emissions is expected when the codelivery and release of both protein and plasmid DNA is successful.

The control experiment (Figure 6a) bombarded with empty, non-DNA coated Au-MSN showed no fluorescence on both green and red channels, as expected. Onion tissue bombarded with Au-MSN loaded with TRITC-BSA and coated with the GFP expression plasmid DNA pLMNC95 showed cells simultaneously fluorescent in red (protein release) and in green (DNA expression) (Figure 6b). Cells bombarded with Au-MSN that was loaded with FITC-BSA and coated with mCherry plasmid DNA showed green fluorescence due to the protein release and red fluorescence due to the DNA expression (Figure 6c). Finally, when eGFP-loaded and mCherry plasmid DNA coated Au-MSN was bombarded into onion tissue, co-localization of both green fluorescent (eGFP release) and red fluorescent (mCherry gene expression) could be detected (Figure 6d), indicating the consistency of the system for the codelivery of both biomolecules. The presence of green fluorescence diffused throughout the entire cell in Figure 6d indicates that the eGFP delivered and released in plant cells remain in the proper configuration. If eGFP denatured or unfolded, then the protein would no longer be fluorescent.[36]

3. Conclusions

We have shown that 10 nm pore-sized, gold functionalized MSN can be used to load proteins with a hydrodynamic diameter as large as 4.5 nm and release them under physiological conditions. The protein-loaded Au-MSN can be subsequently coated with plasmid DNA and introduced into plant tissues through particle bombardment. The delivery and release of two types of biomolecules, protein and plasmid DNA, can be detected in the same plant cells. Further improvements are currently under way to improve protein encapsulation and release efficiencies of MSN materials as well as frequencies for the biolistic delivery in plant tissues. We anticipate that this novel DNA/protein delivery system will lead to advancements in plant cell and plant genomic manipulation applications and research.

4. Experimental Section

Preparation of MSN-10: To synthesize MSN with 10-nm pore size (MSN-10), P104 surfactant (7.0 g) was dissolved in HCl (273.0 g, 1.6 M) and stirred (1 h at 55 °C), followed by rapid addition of tetramethyl orthosilicate (TMOS) (10.64 g). The solution was stirred for 24 h, transferred to a high-pressure vessel and placed in an oven at 150 °C for 24 h. The product was filtered and washed with water and methanol. The surfactant was removed by heating the material to 550 °C for 6 h.

Preparation of Au-MSN: To synthesize $Au(en)_2Cl_3$ for gold modification, ethylenediamine (0.45 mL) was added to an aqueous solution of $HAuCl_4{\cdot}3H_2O$ (1.0 g) in water (10 mL) and stirred for 30 min. Ethanol (70 mL) was added and the $Au(en)_2Cl_3$ precipitate was filtered, washed with ethanol and dried under vacuum. Three cycles of gold functionalization were performed, and for each cycle, $Au(en)_2Cl_3$ (0.372 g) was dissolved in water (150 mL) and the pH adjusted to 10.0 using NaOH. After adding MSN-10 (2.0 g), pH was readjusted to 9.0 with NaOH and stirred for 2 h. The final product (Au-MSN) was filtered and dried under vacuum for 2 days and then, reduced under H_2 flow (150 °C, 3 h).

Fluorescent Labeling of Au-MSN: For FITC labeling, FITC (5 mg, 12.8 μmol) was added to 3-aminopropyltrimethoxysilane (APTMS) (13 μmol) in dry DMSO (0.5 mL), stirred for 30 min and then grafted on to Au-MSN (1.0 g) in toluene. The suspension was refluxed for 20 h under nitrogen and the resulting material was filtered, washed with toluene and methanol, and dried under vacuum overnight.

MSN Surface Area and Porosity Measurement: The surface area and average pore diameter measurements were recorded using nitrogen sorption analysis in a Micromeritics ASAP 2020 BET surface analyzer system. The Brunauer-Emmitt-Teller (BET) and the Barrett-Joyner-Halenda (BJH) equations were used to calculate apparent surface area and pore size distributions, respectively, of MSN samples. Degas of MSN samples were done at 100 °C overnight before analysis.

Zeta Potential Measurements: MSN samples (1 mg) were sonicated in phosphate buffered saline (PBS) pH 7.4 (10 mL), 10 mM NaCl for 5 min and then analyzed on a Zetasizer (Malvern Instruments). The reported zeta potential value is an average of 10 individual measurements. For DNA coated MSN measurements, Au-MSN (1 mg) were coated with ER-rk[38] plasmid (10 μg) and the sample was vigorously shaken to suspend the MSN in the buffer.

Transmission Electron Microscopy (TEM), Scanning Electron Microscopy (SEM), and Scanning Transmission Electron Microscopy (STEM) Imaging: TEM and STEM investigations were done by placing small aliquot of an aqueous suspension on a lacey carbon film coated 400 mesh copper grid and drying it in air. The TEM images were obtained on a Tecnai F^2 microscope. Particle morphology was determined by SEM using a Hitachi S4700 FE-SEM system with 10 kV accelerating voltage.

Protein Loading and In Vitro Release: For protein loading, Au-MSN (20 mg) were sonicated in PBS (5 mL) solution (pH 7.4) followed by the addition of FITC-BSA or TRITC-BSA (Sigma-Aldrich) (15.7 mg). For eGFP (BioVision) encapsulation, Au-MSN (2 mg) and 0.6 mg of the protein were used. The protein-Au-MSN mixture was stirred at room temperature (22 °C) for 24 h and then centrifuged. The supernatant was removed and the remaining MSNs were resuspended briefly in PBS solution (pH 7.4) and lyophilized. To determine protein loading, the fluorescence emission of the FITC-BSA or eGFP in the supernatant was measured using a spectrophotometer. To measure protein release from the Au-MSN, protein-loaded Au-MSN was stirred in PBS (pH 7.4) (2 mL) solution for a period of time. An aliquot was removed and centrifuged to separate the released protein in the supernatant from the MSNs in the pellet, and the fluorescence intensity was measured using at a spectrophotometer (FITC-BSA or eGFP: $\lambda_{Ex} = 488$, $\lambda_{Em} = 518$ nm; TRITC-BSA: $\lambda_{Ex} = 557$, $\lambda_{Em} = 576$ nm).

Plant Materials: White onion epidermis tissue rectangles (2 × 3.5 cm) were placed in dishes containing agar media (0.5 mM 2-(*N*-morpholino)-ethanesulfonic acid (MES), and 15 g L^{-1} of BD Bacto agar, pH 5.7), facing the peeled surface upwards. For tobacco and teosinte leaf bombardment, leaves from 6 to 8 week old in vitro-grown tobacco plants (*Nicotiana tabacum* var. Petite Havana) and leaf pieces of 2-month old teosinte plants (Ames 21785, USDA/ARS/North Central Regional Plant Introduction Station, Iowa State University) were placed with the adaxial surface up on agar media.

Biolistic Method: For the delivery of protein filled Au-MSN, freshly prepared Au-MSN suspensions (5 μl, 20 μg μL^{-1}) in ethanol were loaded onto a macrocarrier. Using a PDS-1000/He biolistic gene gun (BioRad Laboratories), plant samples were bombarded twice at 1350 psi rupture disks and 6 cm target distance. For the delivery of plasmid DNA coated, protein filled Au-MSN, 4 μL of DNA (250 ng μL^{-1}) was added to 10 μL of protein filled Au-MSN (10 μg μL^{-1} stock, freshly prepared in ddH_2O) to make a final ratio of 1 μg DNA to 100 μg Au-MSN per shot. DNA precipitation onto Au-MSN was achieved by adding 12.5 μL of 2.5 M $CaCl_2$ (1 M final concentration) and 5 μL of 0.1 M spermidine (16 mM final concentration) to the DNA/Au-MSN mixture. After mixing the contents, the mixture was briefly centrifuged for 15 s (5000 rpm, room temperature). The supernatant was discarded, the pellet was washed with cold 100% ethanol (60 μL) and centrifuged again. After removal of the supernatant, DNA-coated protein-loaded Au-MSNs were resuspended in cold 100% ethanol (5 μL) and loaded in a macrocarrier. Each plant sample was bombarded twice at 1350 psi and 6 cm target distance.

Fluorescence Microscopy Imaging: Bright field and fluorescence images were taken with 10×A-Plan and or 40×A-Plan objectives of a Zeiss Axiostar plus microscope with a green channel (Endow GFP BP: λ_{ex} = 470 nm, beam splitter = 495 nm and λ_{em} = 525 nm) and a red channel (Texas Red: λ_{ex} = 560 nm, beam splitter = 595 nm and λ_{em} = 645 nm) filters (Chroma Technology Corp.) were used. Microscopy images were taken using ProgRes Capture Pro 2.6 software and a ProgRes C3 digital camera, both from Jenoptik. If necessary, images were edited using Adobe Photoshop software (Adobe Systems Inc).

Supporting Information

Supporting Information is available from the Wiley Online Library or from the author.

Acknowledgements

S.M.-O. and J.S.V. contributed equally to thís work. S.M.-O. and K.W. thank Angela Nguyen for technical support. Mark Millard (NCRPIS/USDA/ARS), Patrick Schnable, and Lisa M. Coffey (Iowa State University) are acknowledged for providing teosinte seeds. This work was partially supported by Plant Sciences Institute of Iowa State University and Pioneer Hi-Bred International, Inc.

Received: February 6, 2012
Revised: April 19, 2012
Published online: May 24, 2012

[1] M.-H. Kim, H.-K. Na, Y.-K. Kim, S.-R. Ryoo, H. S. Cho, K. E. Lee, H. Jeon, R. Ryoo, D.-H. Min, *ACS Nano* **2011**, *5*, 3568.
[2] X. Li, Q. R. Xie, J. Zhang, W. Xia, H. Gu, *Biomaterials* **2011**, *32*, 9546.
[3] F. Torney, B. G. Trewyn, V. S.-Y. Lin, K. Wang, *Nat. Nanotechnol.* **2007**, *2*, 295.
[4] T. Xia, M. Kovochich, M. Liong, H. Meng, S. Kabehie, S. George, J. I. Zink, A. E. Nel, *ACS Nano* **2009**, *3*, 3273.
[5] I. I. Slowing, B. G. Trewyn, V. S.-Y. Lin, *J. Am. Chem. Soc.* **2006**, *128*, 14792.
[6] S. Giri, B. G. Trewyn, M. P. Stellmaker, V. S.-Y. Lin, *Angew. Chem. Int. Ed.* **2005**, *44*, 5038.
[7] S. M. Solberg, C. C. Landry, *J. Phys. Chem. B* **2006**, *110*, 15261.
[8] S. Jung, S. Huh, Y.-P. Cheon, S. Park, *Chem. Commun.* **2009**, 5003.

[9] M. S. Bhattacharyya, P. Hiwale, M. Piras, L. Medda, D. Steri, M. Piludu, A. Salis, M. Monduzzi, *J. Phys. Chem. C* **2010**, *114*, 19928.
[10] J. Ho, M. K. Danquah, H. Wang, G. M. Forde, *J. Chem. Technol. Biotechnol.* **2008**, *83*, 351.
[11] S.-I. Kim, T. T. Pham, J.-W. Lee, S.-H. Roh, *J. Nanosci. Nanotechnol.* **2010**, *10*, 3467.
[12] S. W. Song, S. P. Zhong, K. Hidajat, S. Kawi, *Stud. Surf. Sci. Catal.* **2007**, *165*, 471.
[13] J. L. Vivero-Escoto, I. I. Slowing, B. G. Trewyn, V. S.-Y. Lin, *Small* **2010**, *6*, 1952.
[14] I. I. Slowing, B. G. Trewyn, V. S.-Y. Lin, *J. Am. Chem. Soc.* **2007**, *129*, 8845.
[15] C. J. Staiger, M. Yuan, R. Valenta, P. J. Shaw, R. M. Warn, C. W. Lloyd, *Curr. Biol.* **1994**, *4*, 215.
[16] C. L. Wymer, J. M. Fernandez-Abalos, J. H. Doonan, *Planta* **2001**, *212*, 692.
[17] M. Chang, J.-C. Chou, C.-P. Chen, B. R. Liu, H.-J. Lee, *New Phytologist* **2007**, *174*, 46.
[18] A. Chugh, F. Eudes, *FEBS J.* **2008**, *275*, 2403.
[19] S.-W. Lu, J.-W. Hu, B. R. Liu, C.-Y. Lee, J.-F. Li, J.-C. Chou, H.-J. Lee, *J. Agric. Food Chem.* **2010**, *58*, 2288.
[20] J. Wu, H. Du, X. Liao, Y. Zhao, L. Li, L. Yang, *Plant. Mol. Biol.* **2011**, *77*, 117.
[21] Y. T. Lim, M. Y. Cho, J. M. Lee, S. J. Chung, B. H. Chung, *Biomaterials* **2009**, *30*, 1197.
[22] D. A. Shah, S.-J. Kwon, S. S. Bale, A. Banerjee, J. S. Dordick, R. S. Kane, *Biomaterials* **2011**, *32*, 3210.
[23] B. G. Trewyn, I. I. Slowing, S. Giri, H.-T. Chen, V. S.-Y. Lin, *Acc. Chem. Res.* **2007**, *40*, 846.
[24] J. Liu, F. H. Wang, L. L. Wang, S. Y. Xiao, C. Y. Tong, D. Y. Tang, X. M. Liu, *J. Cent. S. Univ. Technol.* **2008**, *9*, 1007.
[25] Q. Liu, B. Chen, Q. Wang, X. Shi, Z. Xiao, J. Lin, X. Fang, *Nano Lett.* **2009**, *9*, 1007.
[26] S. Martin-Ortigosa, J. S. Valenstein, W. Sun, L. Moeller, N. Fang, B. G. Trewyn, V. S.-Y. Lin, K. Wang, *Small* **2012**, *8*, 413–422
[27] K. Pasupathy, S. Lin, Q. Hu, H. Luo, P. C. Ke, *Biotechnol. J.* **2008**, *3*, 1078.
[28] Q. Wang, J. Chen, H. Zhang, M. Lu, D. Qiu, Y. Wen, Q. Kong, *J. Nanosci. Nanotechnol.* **2011**, *11*, 2208.
[29] A. T. Silva, A. Nguyen, C. Ye, J. Verchot-Lubicz, J. H. J. Moon, *BMC Plant Biol.* **2010**, *10*, 291.
[30] V. Grichko, V. Grishko, O. Shenderova, *NanoBioTechnology* **2006**, *2*, 37.
[31] E. Wild, K. C. Jones, *Environ. Sci. Technol.* **2009**, *43*, 5290.
[32] H. Zhu, C. Liang, W. Yan, S. H. Overbury, S. Dai, *J. Phys. Chem. B* **2006**, *110*, 10842.
[33] U. Böhme, U. Scheler, *Chem. Phys. Lett.* **2007**, *435*, 342.
[34] M. A. Hink, R. A. Griep, J. W. Borst, A. Van Hoek, M. H. M. Eppink, A. Schots, A. J. W. G. Visser, *J. Biol. Chem.* **2000**, *275*, 17556.
[35] A. Katiyar, L. Ji, P. G. Smirniotis, N. G. Pinto, *Microporous Mesoporous Mater.* **2005**, *80*, 311.
[36] W. W. Ward, S. H. Bokman, *Biochemistry* **1982**, *21*, 4535.
[37] S. S. Bale, S. J. Kwon, D. A. Shah, A. Banerjee, J. S. Dordick, R. S. Kane, *ACS Nano* **2010**, *4*, 1493.
[38] B. K. Nelson, X. Cai, A. Nebenführ, *Plant J.* **2007**, *51*, 1126.
[39] S. L. Mankin, W. F. Thompson, *Plant Mol. Biol. Reporter* **2001**, *19*, 13.